Adsorption Rate Studies—Significance of Pore Diffusion

SHINOBU MASAMUNE and J. M. SMITH

University of California, Davis, California

Adsorption rates were measured by a transcient method for nitrogen on beds of porous Vycor glass particles. Nitrogen was adsorbed, from a low concentration in helium, at liquid nitrogen temperature.

Equations are presented for the concentration as a function of time and position in the bed, based upon surface adsorption, pore diffusion, or external diffusion controlling the overall process. Analysis of the data with these results indicates that the surface adsorption is a very rapid process and that pore processes determine the rate for particles larger than 0.01 cm. in radius. The effective pore diffusivity was determined to be 0.04 sq. cm./sec. The predominant contribution to the diffusivity is a surface mechanism rather than diffusion in the gas within the pores.

Adsorption rates on porous solids are of significance in separation processes, such as drying and hydrocarbon fractionation, and in heterogeneous catalytic reactions. Measured from concentrations in the fluid surrounding the porous particle, these rates reflect the relative resistances of the adsorption step on the solid surface, diffusion in the pores including surface diffusion, and diffusion (external) from the outer surface of the particle into the fluid stream. For physical adsorption activation energies are only a few thousand calories (per gram mole), so that diffusion resistances may be the controlling factor in establishing the measured rate. Little work has been done apparently to compare these three resistances in a quantitative fashion. However Geser and Canjar (*10*) have obtained data, for the low-temperature adsorption of methane in hydrogen on activated carbon, which suggest that the surface process is of negligible resistance with respect to the diffusion steps. The objective of the present paper is to analyze quantitatively adsorption data by comparison with rate equations based upon the three steps in the overall process. In this way the controlling resistance can be ascertained.

A transient method was used to measure low-temperature adsorption rates for nitrogen on Vycor glass. Since the effect of particle size on the resistance of each of the three steps is different, the diameter of the Vycor particle was the major variable in the experimental work.

The results of comparing theory with experiment show that the pore processes controlled the rate for the authors' system. Hence the data could be used to evaluate an effective diffusivity for nitrogen in Vycor. A secondary objective of the work was to compare this diffusivity with results obtained from direct diffusion measurements. This procedure provided some information on the importance of surface diffusion.

In the experimental procedure a mixture of nitrogen and helium was passed through a fixed bed of Vycor particles, and the concentration of nitrogen leaving the bed was measured as a function of time. To relate these results to the surface and pore processes requires equations which express the concentration as a function of time and position, first for a single particle in the bed and second for the bed as a whole. Edeskuty and Amundson (*7*), Rosen (*16*), and Thomas (*20*) have treated the mathematical aspects of the problem when pore resistances are significant, and their work has been valuable in interpretating the data. In the next section equations are given for three cases, corresponding to surface adsorption, pore processes, and external diffusion controlling the overall process.

THEORETICAL DEVELOPMENT

Imagine a packed bed of spherical particles (radius = a) of length z_o maintained at constant temperature and through which flows a nitrogen-helium system, of nitrogen concentration C_o, at a constant velocity u. The system is at a temperature such that no adsorption occurs until time $t = 0$ when the temperature is reduced to −196°C. (liquid nitrogen temperature).

The interparticle concentration C in the bed is related to the time and bed length by the expression

$$u\left(\frac{\partial C}{\partial z}\right) + \epsilon_B \frac{\partial C}{\partial t} + \tilde{R} = 0 \qquad (1)$$

In equation (1) radial and longitudinal diffusion terms are not included since they are negligible and $\tilde{R}$ is the overall rate of nitrogen adsorption per unit volume of bed. The boundary conditions are

$$\begin{cases} C = \overline{C} = 0 \text{ at } t = 0 \ z \geqslant 0 \\ \overline{q} = 0 \end{cases} \qquad (2)$$

$$C = C_o \text{ at } z = 0, \ t \geqslant 0 \qquad (3)$$

where $\overline{C}$ and $\overline{q}$ are the intraparticle concentrations in the pore space and on the pore surface, respectively.

The local rate of adsorption on the pore surface is assumed to be proportional to the concentration $\overline{C}$ of nitrogen in the gas and to the bare surface of the adsorbent. If $\overline{q}$ is the concentration of nitrogen on the solid surface, expressed per unit mass of adsorbent and S the surface per unit mass, the bare surface per unit mass is given by $\frac{1}{q_\infty} S (q_\infty - \overline{q})$. Here q_∞ is the total adsorption capacity corresponding to a monomolecular layer of nitrogen on the surface. The rate of desorption in similar terms is pro-

portional to the occupied surface, or $\frac{1}{q_\infty}\bar{q}S$. Hence the net local rate of adsorption at a point on the pore surface, per unit mass of adsorbent, is

$$R = kS\left[\bar{C}(q_\infty - \bar{q}) - \frac{1}{K}\bar{q}\right] \tag{4}$$

where k is the rate constant for adsorption per unit surface divided by q_∞. The concentration $\bar{q}$ and $\bar{C}$ are functions of r (particle radius) when pore resistances are important and independent of r when they are not important.

At equilibrium conditions, and for $\bar{C} = C_o$, Equation (4) gives the equilibrium value of $\bar{q}$ as follows:

$$\bar{q}_o = \frac{Kq_\infty C_o}{1 + KC_o} \tag{5}$$

When the concentration C_o is low enough, the equilibrium relationship between $\bar{q}_o$ and C_o is linear. That is Equation (5) becomes

$$\bar{q}_o = Kq_\infty C_o = \lambda_e C_o$$

In the experimental work of this study the concentration C_o was small enough that this expression was valid. For other concentrations in the linear range the equilibrium equation takes the form

$$\bar{q} = \lambda_e \bar{C} \tag{6}$$

Surface Adsorption Rate Controlling

The solution for the concentration as a function of time at the exit of the bed ($z = z_o$) for the case of irreversible adsorption was obtained by early investigators (*5, 18*). For reversible adsorption the net rate as given by Equation (4) is a function of time but uniform throughout the pore surface, since the concentrations $\bar{C}$ and $\bar{q}$ are constant. Converted to a basis of a unit volume of bed this rate $\tilde{R}$ for the particle is given by the expression

$$\tilde{R} = \rho_B(kS)\left[\bar{C}(q_\infty - \bar{q}) - \frac{1}{K}\bar{q}\right] \tag{7}$$

The solution of Equations (1 to 3) and (7) was presented by Thomas (*19*) and converted into a more useful form by Hiester and Vermeulen (*12*). Their result may be written as

$$\frac{C_o}{C} = 1 + \frac{\pi^{1/2}\{1 - \text{erf}\,(\sqrt{P_1P_3} - \sqrt{P_2})\}\exp(\sqrt{P_1P_3} - \sqrt{P_2})^2}{\pi^{1/2}\{1 - \text{erf}\,(\sqrt{P_1P_2} - \sqrt{P_3})\}\exp(\sqrt{P_1P_2} - \sqrt{P_3})^2} \frac{-[\sqrt{P_1P_3} + (P_1P_2P_3)^{1/4}]^{-1}}{+[\sqrt{P_3} + (P_1P_2P_3)^{1/4}]^{-1}} \tag{8}$$

where

$$P_1 = \frac{1}{KC_o + 1}\begin{pmatrix}\text{for linear equilibrium}\\ P_1 = 1\end{pmatrix} \tag{9}$$

$$P_3 = kSC_o\frac{q_\infty}{q_o}\left(t - \frac{z_o\epsilon_B}{u}\right) \tag{10}$$

$$P_2 = \frac{kSq_\infty z_o\rho_B}{u} \tag{11}$$

Pore Diffusion Processes Controlling

For this case the rate $\tilde{R}$ must be expressed in terms of the geometrical properties of the particle and then combined with Equation (1) to obtain the concentration $C = f(t)$ at $z = z_o$. The rate can be written in terms of an effective diffusivity D_i as follows:

$$\tilde{R} = 4\pi a^2 \bar{n} D_i\left(\frac{\partial \bar{C}}{\partial r}\right)_{r=a} \tag{12}$$

The number of spheres per unit volume of bed $\bar{n}$ is given by

$$\bar{n} = \frac{3(1 - \epsilon_B)}{4\pi a^3} = \frac{3\rho_B}{4\pi a^3 \rho_p} \tag{13}$$

Combining these expressions one gets

$$\tilde{R} = \frac{3\rho_B}{\rho_p}\left(\frac{D_i}{a}\right)\left(\frac{\partial \bar{C}}{\partial r}\right)_{r=a} \tag{14}$$

The gradient in Equation (14) can be determined by differentiating the function $\bar{C} = f(t, r)$ for the particle. The differential form of this function is obtained from a mass balance of nitrogen on a spherical shell of the particle of radii r and $r + \Delta r$. The result is

$$D_i\left(\frac{\partial^2 \bar{C}}{\partial r^2} + \frac{2}{r}\frac{\partial \bar{C}}{\partial r}\right) = \epsilon_p\frac{\partial \bar{C}}{\partial t} + \rho_p\frac{\partial \bar{q}}{\partial t} \tag{15}$$

where the effective diffusivity D_i is dependent upon the pore structure as well as surface and gas diffusion.

Since pore diffusion processes are assumed to be controlling, local equilibrium exists between gas and pore surface. Hence Equation (7) relates $\bar{q}$ and $\bar{C}$. Combining this with Equation (15) one gets

$$\frac{D_i}{\epsilon_p + \lambda_e\rho_p}\left(\frac{\partial^2 \bar{C}}{\partial r^2} + \frac{2}{r}\frac{\partial \bar{C}}{\partial r}\right) = \frac{\partial \bar{C}}{\partial t} \tag{16}$$

Edeskuty and Amundson (*7*) solved the problem represented by Equations (1), (2), (3), (14), and (16) including the effect of external diffusion resistance. This was handled by the boundary condition

$$D_i\left(\frac{\partial \bar{C}}{\partial r}\right)_{r=a} = k_f(C - C) \tag{17}$$

Their solution in terms of the Laplace transform of $C(\theta, x)$ is

$$L[C(x,\theta)] = \int_o^\infty e^{-s\theta}C(x,\theta)d\theta = \frac{C_o}{s}e^{-Y(s)x} \tag{18}$$

where

$$Y(s) = \left[\frac{3\rho_B D_i}{\epsilon_B \rho_p a^2}\right] \frac{\sin W(s) - W(s)\cos W(s)}{\left(\frac{D_i}{k_f\alpha} - 1\right)\sin W(s) - \frac{D_i}{k_f a}W(s)\cos W(s)} \tag{19}$$

and

$$W(s) = a\,i\left(s\frac{\epsilon_p + \lambda_e\rho_p}{D_i}\right)^{1/2} \tag{20}$$

For the case considered in this section, external diffusion is neglected, so that Equation (19) reduces to

$$Y(s) = \frac{3\rho_B D_i}{\epsilon_B \rho_p a^2}[W(s)\cot W(s) - 1] \tag{21}$$

The desired solution is the inverse transform of Equation (18), which may be written as the contour integral

$$\frac{C(x,0)}{C_o} = \frac{1}{2\pi i}\int_{\delta-\infty}^{\delta+\infty}\frac{1}{s}(e^{s\theta - Y(s)x})\,ds \tag{22}$$

In Equations (18) and (22) x and θ are new variables related to distance z and time (t) as follows:

$$x = \frac{z\,\epsilon_B}{u} \tag{23}$$

$$\theta = t - \frac{z\,\epsilon_B}{u} \tag{24}$$

Rosen (*16*) has simplified the evaluation of Equation (22) by transforming it into a real integral which may be represented by the following equations:

$$\frac{C(x,\theta)}{C_o} = \frac{1}{2} + \frac{2}{\pi}\int_o^\infty \frac{\exp(-\gamma x H_{D1}(\lambda)\sin[\alpha\theta\lambda^2 - \gamma x H_{D2}(\lambda)]}{\lambda}\,d\lambda \tag{25}$$

where the integration parameter λ, $H_{D1}(\lambda)$, $H_{D2}(\lambda)$, α, and γ are

$$H_{D1}(\lambda) = \frac{\lambda(\sinh 2\lambda + \sin 2\lambda)}{\cosh 2\lambda - \cos 2\lambda} - 1 \tag{26}$$

$$H_{D2}(\lambda) = \frac{\lambda(\sinh 2\lambda - \sin 2\lambda)}{\cosh 2\lambda - \cos 2\lambda} \tag{27}$$

$$\alpha = \frac{2}{\epsilon_p + \lambda_e \rho_p}\left(\frac{D_i}{a^2}\right) \approx \frac{2}{\lambda_e\,\rho_p}\left(\frac{D_i}{a^2}\right) \tag{28}$$

$$\gamma = \frac{3(1-\epsilon_B)}{\epsilon_B}\left(\frac{D_i}{a^2}\right) = \frac{3\,\rho_B}{\epsilon_B\,\rho_p}\left(\frac{D_i}{a^2}\right) \tag{29}$$

The approximation in Equation (28) is justified since the ratio $\epsilon_p/\lambda_e\rho_p$ is less than 0.001 for the experimental conditions of this study. Rosen's functions, Equations (27) and (28), are bounded; both approach zero as λ approaches zero and become $\lambda - 1$ and λ, respectively, at high values of λ.

The important feature of these equations is the group D_i/a^2. The value of Equation (25) is sensitive to small variations in this group, indicating that particle size has a strong effect on $C(x,\theta)$ provided pore diffusion is important. Numerical evaluation of Equation (25) is considered in another section.

External Diffusion Controlling

For this case equilibrium is established between $\overline{C}$ and $\overline{q}$ as given by Equation (6). Also the rate of adsorption $\tilde{R}$ is determined by the concentration difference $(\overline{C} - C)$ between the particle surface and the gas stream. This can be expressed in terms of the mass transfer coefficient at the surface k_f:

$$\tilde{R} = \overline{n}\,4\pi a^2 k_f\,(C - \overline{C}) = \frac{3\,\rho_B}{\rho_p}\frac{k_f}{a}\left(C - \frac{\overline{q}}{\lambda_e}\right) \tag{30}$$

where the last equality is obtained by using Equations (6) and (13). The value of k_f can be estimated from empirical correlations of packed bed data such as that of Hougen, Gamson, and Thodos (*9*). Their results may be written in the form

$$k_f = \frac{u}{\beta}\,(N_{Re})^{-0.51}\,(N_{Sc})^{-2/3} \tag{31}$$

where β is a constant equal to 1/1.82 for modified Reynolds' numbers less than 350.

Equations (1), (2), (3), and (30) were solved by Anzelius (*1*), Schumann (*17*), Furnas (*8*), and more recently by Pigford and Marshall (*14*). The result is

$$\frac{C}{C_o} = 1 - e^{-q_2 t}\int_o^{q_1 z} e^{-q_1 z}\,J_o\,(2i\sqrt{(q_1 z)\,(q_2 t)})\,d(q_1 z) \tag{32}$$

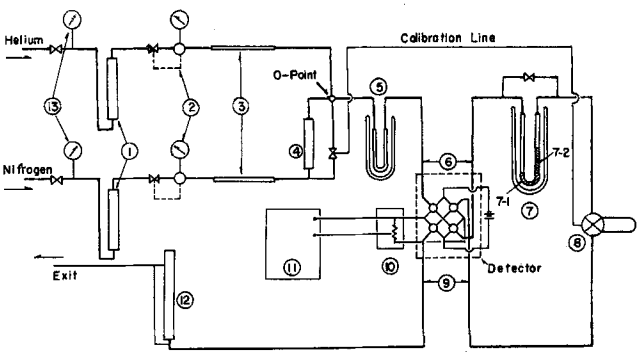

Fig. 1. Schematic diagram of apparatus.

where

$$q_1 = \frac{3\,\rho_B}{a\,\beta\,\rho_p}\,(N_{Re})^{-0.51}\,(N_{Sc})^{-2/3} \tag{33}$$

$$q_2 = \frac{uq_1}{\rho_B\,\lambda_e} = \frac{3u}{\rho_p\,\lambda_e\,\beta a}\,(N_{Re})^{-0.51}\,(N_{Sc})^{-2/3} \tag{34}$$

Equation (32) is compared with the data in another section.

EXPERIMENTAL

A shell sorptometer with some modifications (*2*) was used for both the equilibrium and kinetic studies. Figure 1 is a flow diagram of the apparatus. Nitrogen and helium (both of 99.99 wt. % purity) entered the apparatus at constant flow rates, maintained by automatic pressure control valves (2) and lengths of restricted-diameter tubing (3). Each gas was passed through a separate bed (1) of silica gel to remove small amounts of residual water. After mixing at point O the gases flow through a cold trap (5) at liquid nitrogen temperature and thence to the reference side of the detector cell (6). The detector consisted of a four filament (tungsten) thermal conductivity cell. The cell was of the straight up, convection type with a time lag of 2 to 3 sec. The entire cell was contained in a constant-temperature water bath. Leaving the cell the gas mixture enters a precooler bed (7-1) consisting of 3 cm. of 470-μ diam. glass beads (nonporous). Immediately after the precooler is the sample bed (7-2) of Vycor glass particles. Both beds are in glass tubing having an inside diameter of 0.460 ± 0.005 cm. Leaving the bed the gas enters the sample side (9) of the detector and then is discharged via the soap film meter (12).

The small nitrogen flow rate was measured with an especially accurate rotameter (4) in the line prior to the mixing point (0). The electromotive force from the cell is fed to the potentiometer recorder (11) through the attenuator (10). At maximum sensitivity 1 millivolt (mv.) corresponded to full scale (10 in.) deflection on the recorder. All the connecting gas lines were made of ¼-in. copper tubing. The capillary restriction for nitrogen was 0.01-in. I.D. stainless steel tubing, and for helium various sizes of glass capillaries were used, depending upon the flow rate. For calibration a known amount of pure nitrogen could be introduced into the apparatus via the O-tubing (8) connected to the main line.

A possible source of error in the work is diffusion of nitrogen in the tubing (also 0.460-cm. I.D.) between the detector (9) and the exit of the Vycor bed (7-2). The concentration given in the equations in the preceeding section refer to the exit of the bed. Hence any change in concentration between this point and the detector introduces an error. The magnitude of this diffusion was measured and the results are discussed in the Appendix.* It is shown there that the dispersion error is negligible under the experimental conditions employed, except possibly for the bed of smallest particles of Vycor (a = 0.0099 cm.) where the overall rate is very high.

Tabular material has been deposited as document 7821 with the American Documentation Institute, Photoduplication Service, Library of Congress, Washington 25, D. C., and may be obtained for $1.25 for photoprints or for 35-mm. microfilm.

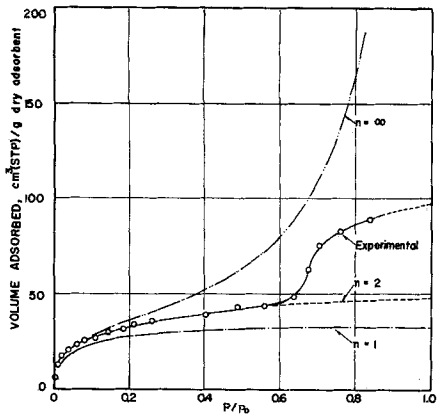

Fig. 2a. Equilibrium adsorption curve.

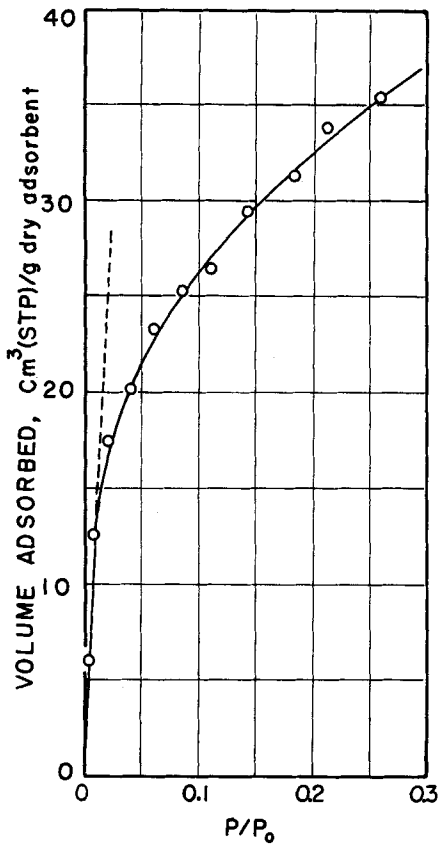

Fig. 2b. Equilibrium adsorption curve, low range.

Table 1. Properties of Vycor Glass

Surface area, S	141 sq. m./g.
Void volume, V	0.177 cc./g.
Void fraction, ϵ_p	0.256
Average pore radius, $\bar{r}$	25Å ($\bar{r} = 2V/S$)
True density, ρ	1.95 g./(cc.)
Particle density*, ρ_p	1.45 g./(cc.)

* Supplied by manufacturer.

Table 2. Properties of Vycor Beds

Bed no.	Particle size U.S. sieve range	Particle size Average radius, a, cm.	Void fraction ϵ_B	Bed density ρ_B, g./(cc.)	(D_i/a^2)* sec.$^{-1}$
1	10-14	0.0793	0.447	0.802	6.35
2	16-20	0.0463	0.447	0.802	18.7
3	40-60	0.0151	0.447	0.802	176
4	60-80	0.0099	0.447	0.802	407

* Based upon $D_i = 0.04$ sq. cm./sec.

Properties of Vycor Glass

The nitrogen adsorption isotherm for the Vycor used is shown in Figures 2*a* and 2*b*. These data were obtained in the sorptometer with the sample at liquid nitrogen temperature. From the experimental data surface area, void volume, and related properties were determined. The results are given in Table 1. The isothem is of type IV [classification of Brunauer (6)] suggesting that the pore size distribution is relatively narrow up to approximately $p/p_o = 0.6$ and that only a limited number of molecular layers (n) of nitrogen are adsorbed up to this pressure ratio. Calculated adsorption data based upon the general Bennett-Emmet-Teller equation (*6, 13*) are shown in Figure 2*a* for $n = 1$, $n = 2$, and $n = \infty$. The enlarged plot of the low range of the data shown in Figure 2*b* indicates that the equilibrium curve [Equation (6)] is linear up to p/p_o of 0.01.

Properties of Bed Vycor Particles

Vycor glass obtained in cylindrical rods ½ in. in diameter was fractured, ground, and separated by conventional sieve analysis. Four separate fractions were studied and the properties of these four beds are shown in Table 2. Before adsorption data was taken, the Vycor was dehydrated by heating to 180°-220°C. for 2 hr. in a stream of helium.

Operating Procedure

Before initiation of adsorption the precooler and sample bed were purged with the operating mixture of helium and nitrogen for about 30 min. at room temperature. Then adsorption was initiated by immersing the beds in a liquid nitrogen bath. This instant was recorded as $t = 0$, and the adsorption curve was recorded as a function of time. Judging from the curve (for example, see Figure 3) the time required to approach thermal equilibrium was less than 5 sec. This time lag is of

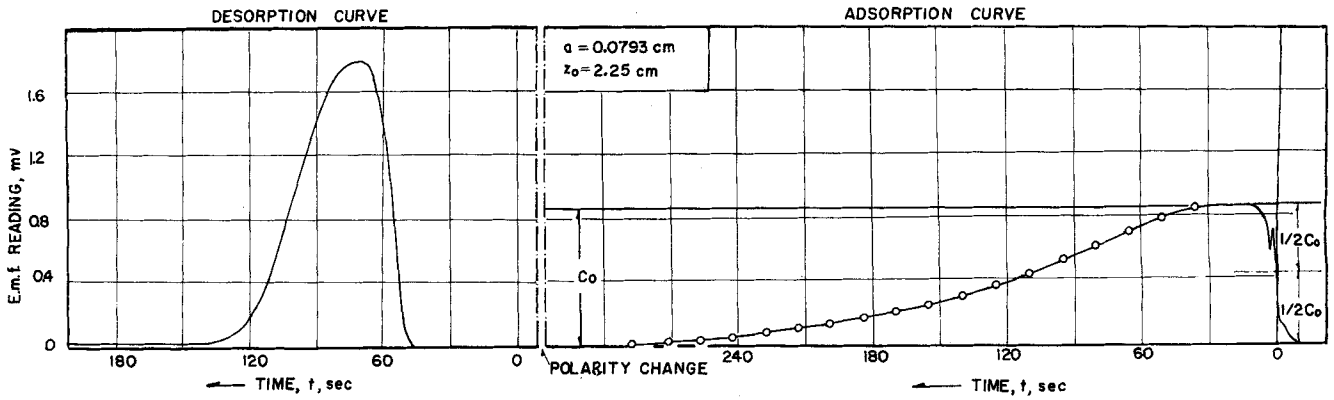

Fig. 3. Illustrative adsorption and desorption curves.

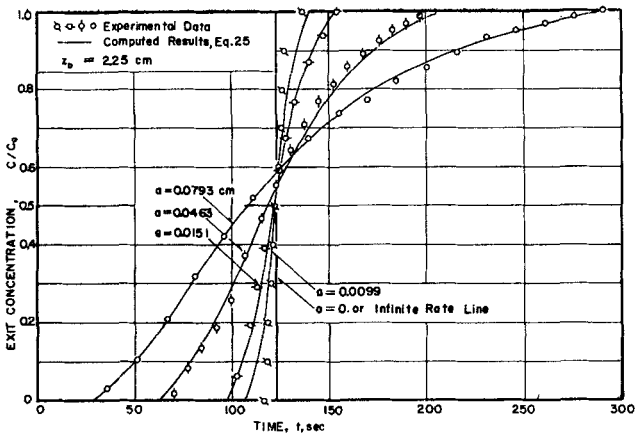

Fig. 4. Experimental data and computed results, intraparticle diffusion controls rate.

negligible magnitude with respect to the time for adsorption. However in analyzing the data corrections were made for the holdup time in the volume between exit of bed and the reactor. The run was terminated after the exit concentration again attained the feed concentration. The type of curve obtained is illustrated in Figure 3 for a bed (length 2.25 cm.) made using particles 0.0793 cm. in radius. For this run the exit concentration decreased to zero a few seconds after immersion of the bed in the liquid nitrogen bath. The breakthrough curve is observed to start at about 30 sec. and complete adsorption achieved after about 290 sec., at which point the exit concentration has returned to its initial value. Also shown in Figure 3 is the corresponding desorption curve obtained when the liquid nitrogen bath was removed from around the bed.

Scope of Data

The chief variable in the kinetic measurements was particle radius, although data for somewhat different bed lengths were also obtained. Breakthrough curves, similar to Figure 3, were measured for the following conditions:

Temperature: −196°C. (liquid nitrogen)
Vycor particle radius: 0.0793, 0.0463, 0.0151, and 0.0099 cm.
Flow rate: 183.1 cc./min. [at standard pressure and temperature (STP)] or a superficial velocity of 18.5 cm./sec.
Total pressure: atmospheric
Bed length: z_o = 2.25, 2.70, and 3.15 cm.
Nitrogen concentration: p/p_o = 0.01 ± 0.0005
Bed density: ρ_B = 0.802 g./cc.; void fraction, ϵ_B = 0.447

ANALYSIS OF DATA

Figure 4 shows corrected adsorption results, obtained from data as illustrated in Figure 3 and plotted as C/C_o vs. time. The experimental data for each particle size are indicated as circles and identified with the proper a value. In each case the bed length was 2.25 cm. (300 mg. of particles). The vertical line on the graph indicates the time t_s required for C/C_o to increase to unity, if the overall rate of adsorption were infinite. This time is that needed for sufficient nitrogen to flow into the bed for the Vycor particles to reach equilibrium with a gas concentration of C_o. Hence the following mass balance gives t_s:

$$t_s\,(u\,C_o)\,A_c = \rho_B\,\overline{q_o}\,(A_c\,z_o) = \rho_B\,\lambda_e\,C_o\,A_c\,z_o$$

or

$$t_s = \frac{\rho_B\,\lambda_e\,z_o}{u} = \frac{(0.802)\,(1{,}260)\,(2.25)}{18.5} = 123 \text{ sec.}$$

The data in Figure 4 show that the particle size has a significant effect on the slope of the breakthrough curves and hence on the adsorption rate. Also the overall rate is seen to be very rapid for the smallest particle; that is the data points for a = 0.0099 cm. form a curve very close to the vertical line.

Surface Adsorption Resistance

Equation (8), for the case of surface adsorption resistance controlling the overall rate, suggests no effect of particle size and hence cannot fit the data points shown in Figure 4. Equation (8) in this respect simply expresses the known fact that the surface area, in porous solids with large areas, is independent of particle size. Thus the data in Figure 4 indicate that the surface adsorption rate for nitrogen on Vycor particles is comparatively rapid. Hence the resistance of the surface process is negligible with respect to that of the other steps in the overall adsorption, except perhaps for the case of the smallest particle (a = 0.0099 cm.).

External Diffusion Resistance

Equation (32) gives C/C_o as a function of time for the case in which the external diffusion step controls the overall process. Values of C/C_o calculated from Equation (32) are shown in Figure 5 for the four particle sizes studied. Also shown on the figure, as circles, are the experimental data for the largest and smallest particles. It is clear that the observed effect of particle radius is much larger than that predicted from Equation (32). Also the overall rate for the smallest particle is greater (the line is nearly vertical) than the predicted line for this value of a. The opposite result would be expected since the actual data include the resistances due to pore processes and the surface rate. It is concluded that the mass transfer resistances predicted from Equation (31) are too high, presumably owing to the low Reynolds number or small particle size compared with the conditions for which Equation (31) was determined.

Pore and Surface Diffusion Resistances

From the foregoing analysis it appears that the pore processes are an important resistance. If this step controls the adsorption rate, Equation (25) should fit the data. Furthermore the diffusivity D_i should be constant with respect to particle size and bed length. Accordingly this hypothesis was tested in the following manner.

1. Evaluation of D_i. From the breakthrough data for the largest particle (a = 0.0793 cm.) the optimum value of D_i was determined by comparison with curves calculated from Equation (25). The computations were carried out with an IBM-1410 computer. The results are shown in Figure 6. The data agree well for D_i = 0.040 sq.cm./sec. with an error range of about ± 0.005 sq. cm./sec.

2. Constancy of D_i. With D_i = 0.04 breakthrough curves were computed for the three other particle sizes from Equation (25). The results are given in Figure 4, where the com-

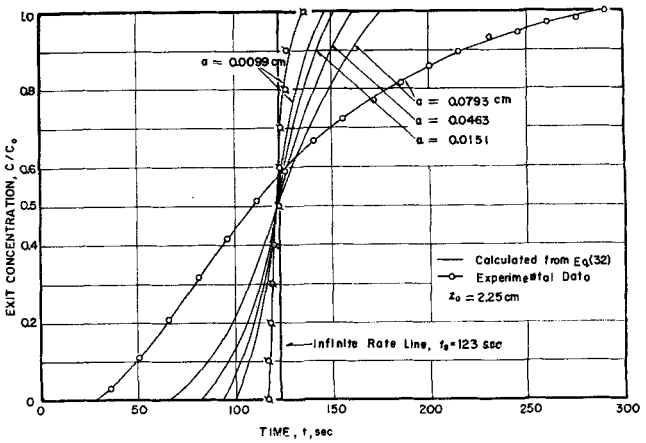

Fig. 5. Computed breakthrough curve, external diffusion controls rate.

puted curves are compared with the experimental data. For all but the smallest particle size the computed and experimental results agree well, lending confidence to the value of D_i and substantiating the hypothesis that pore resistances control the overall adsorption rate. For the smallest particle the agreement is not good. It may be that for these small particles the diffusion path length is too small for pore processes to control the overall adsorption rate. Also the rate is so high for this particle size that the accuracy of the data decreases. In addition diffusion in the line between detector and exit of bed could introduce a small error for this particle size (see Appendix).*

3. Effect of bed length. To test further the pore resistance hypothesis experimental data were obtained for Vycor beds of different length but all made with particles of radius $a = 0.0463$ cm. The data and computed results from Equation (25) are shown in Figure 7. In view of the random errors associated with repacking the bed and accurate measurement of its length the agreement is good.

For the conditions of this study it is concluded that intraparticle diffusion processes control the adsorption of nitrogen on Vycor for particles larger than 0.01-cm. radius. It is now of interest to examine the numerical magnitude of the effective diffusivity in terms of surface and gas diffusion mechanisms.

Surface and Pore Diffusion

The diffusivity D_i determined above represents the combined contributions of two-dimensional surface diffusion on the pore walls (surface diffusivity D_s) and the usual gas diffusion in the pore volume (pore diffusivity D_p). Glueckauf (*11*) and Barrer (*3, 4*) considered the quantitative description of surface diffusion, and Barrer wrote separate mass balance equations for each contribution. In a similar way one may write

$$D_s \rho_p \left(\frac{\partial^2 \bar{q}}{\partial r^2} + \frac{2}{r} \frac{\partial \bar{q}}{\partial r} \right) = \rho_p \frac{\partial \bar{q}}{\partial t} \qquad (35)$$

$$D_p \left(\frac{\partial^2 \bar{C}}{\partial r^2} + \frac{2}{r} \frac{\partial C}{\partial r} \right) = \epsilon_p \frac{\partial \bar{C}}{\partial t} \qquad (36)$$

For the conditions of the present work it has been shown that equilibrium is reached between the nitrogen concentration on the surface q and that in the gas $\bar{C}$, in accordance with Equation (6). With this restraint Equation (35) becomes

$$D_s \rho_p \lambda_e \left(\frac{\partial^2 \bar{C}}{\partial r^2} + \frac{2}{r} \frac{\partial \bar{C}}{\partial r} \right) = \rho_p \lambda_e \frac{\partial \bar{C}}{\partial t} \qquad (37)$$

* See footnote on page 248.

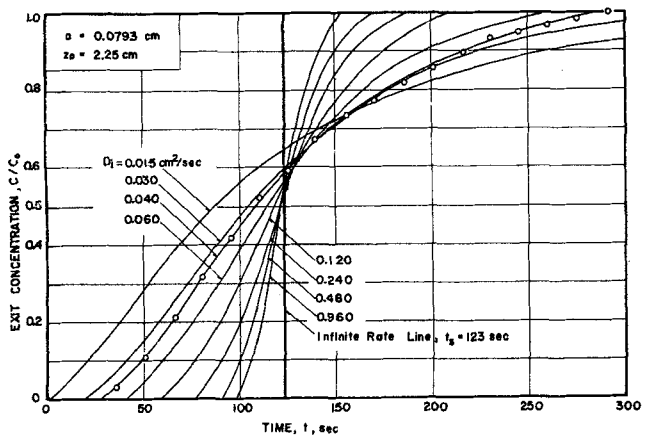

Fig 6. Evaluation of intraparticle diffusivity D_i.

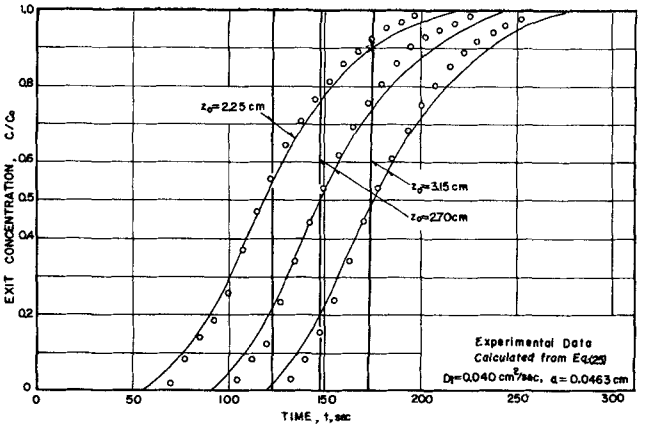

Fig. 7. Effect of bed length on breakthrough curves.

Addition of Equations (36) and (37) gives a combined equation in terms of the sum of the surface and gas diffusivities:

$$\frac{D_p + \rho_p \lambda_e D_s}{\epsilon_p + \lambda_e \rho_p} \left(\frac{\partial^2 \bar{C}}{\partial r^2} + \frac{2}{r} \frac{\partial \bar{C}}{\partial r} \right) = \frac{\partial \bar{C}}{\partial t} \qquad (38)$$

Barrer introduces a Henry's law coefficient equal to λ_e/S, where S is related to the average pore radius by $2V/\bar{r}$ or $2\epsilon_p/\rho_p$. Also he considers diffusion in a single capillary rather than in a spherical particle of porosity ϵ_p. With these two modifications considered Equation (38) is identical to that proposed by Barrer.

Comparison of Equations (16) and (38) shows that the measured diffusivity D_i is

$$D_i = D_p + \rho_p \lambda_e D_s \qquad (39)$$

Rao and Smith (*15*) have measured diffusivities of several gases in the same Vycor glass used in this study, and the value for nitrogen at 20°C. is $D_i = 3.6 \times 10^{-4}$. Barrer (*3*) estimates that 68% of this value is surface diffusion at room temperature. Hence the pore gas diffusivity D_p is estimated to be $(1 - 0.68)(3.6 \times 10^{-4})$ or 1.1×10^{-4} sq. cm./sec. In Vycor with $\bar{r} = 25$Å the diffusion is of the Knudsen type for which the diffusivity is proportional to $T^{1/2}$. Hence at liquid nitrogen temperature $D_p = 5.7 \times 10^{-5}$ sq. cm./sec. With $D_i = 0.04$ sq. cm./(sec.) Equation (39) shows the surface contribution is dominant at −196°C. Since $\rho_p = 1.45$ g./cc. and $\lambda_e = 1{,}260$ cc./g., D_s can be approximated as follows:

$$D_s = \frac{D_i - D_p}{\rho_p \lambda_e} = \frac{0.040 - 5.75 \times 10^{-5}}{1.45\ (1{,}260)}$$

$$= 2.2 \times 10^{-5} \text{ sq. cm/sec.}$$

From this result and the value of D_s at 20°C. it is possible to predict a rough figure for the heat of adsorption of nitrogen on Vycor in the low p/p_o region (that is monomolecular layer). This was done by taking λ_e and D_s as the following functions of temperature:

$$\lambda_e = \lambda_e^o \exp(-\Delta H/RT) \qquad (40)$$

$$D_s = A \exp(-E/RT) \qquad (41)$$

On the assumption that $E = 1{,}600$ cal./g. mole as the activation energy for surface diffusion of nitrogen, as suggested by Barrer, ΔH calculated from Equation (39) applied at 20°C. and at liquid nitrogen temperature is − 2,060 cal./g. mole. This appears to be a reasonable value for the heat of adsorption.

It is included that at low temperatures intraparticle diffusion is mainly of the surface type. Also the high value of $D_i = 0.04$ sq. cm./sec. is due to the increase of the adsorption equilibrium constant with decrease in temperature.

ACKNOWLEDGMENT

The authors would like to acknowledge the financial support of the United States Army Research Office (Durham) through Grant #DA-ARO(D)-31-124-G191.

NOTATION

a = average radius of Vycor particles, cm.
C = interparticle nitrogen concentration, g.moles/(cc. of nitrogen-free helium)
$\bar{C}$ = intraparticle nitrogen concentration, g.moles/(cc. of nitrogen-free helium)
C_o = nitrogen concentration at bed inlet, g.moles/cc.
D_i = total effective diffusivity within particle, based upon the spherical area perpendicular to radial direction, sq. cm./(sec.)
D_p = effective diffusivity in the gas space of the pores, based upon the spherical area perpendicular to radial direction, sq. cm./(sec.)
D_s = surface diffusivity on pore walls, based upon the spherical area perpendicular to radial direction, sq. cm./(sec.)
D_{NH} = molecular diffusivity of nitrogen-helium system, sq. cm./(sec.)
$\bar{D}_z$ = axial diffusivity in tubing between exit of bed and detector, sq. cm./(sec.)
E = energy of activation for surface diffusion, cal./(g. mole)
u = velocity of nitrogen-free helium based upon area of empty bed, cm./(sec.), this velocity is the same as that in the tubing between bed and detector
ΔH = heat of adsorption, cal./(g. mole)
H_{D1}, H_{D2} = Rosen's functions given by Equations (26) and (27)
i = imaginary quantity
K = adsorption equilibrium constant, cc./(g. mole)
k = adsorption rate constant per unit surface area of pores, g.(cm.)/(g. mole) (sec.)
k_f = external mass transfer coefficient based upon external surface of particle and concentration driving force, cm./(sec.)
L = length of U tube used for adding nitrogen, cm.
N_{Re} = modified Reynolds/number, $(2a\,u\rho/\mu)$
N_{Sc} = Schmidt number, $\mu/\rho\,D_{NH}$
n = number of layers of molecules of nitrogen adsorbed on Vycor surface
$\bar{n}$ = number of Vycor particles per unit volume of packed bed, cm.$^{-3}$
p/p_o = nitrogen pressure expressed as fraction of saturation pressure, p/p_o
P_1, P_2, P_3 = functions defined by Equations (9) to (11)
$\bar{q}$ = intraparticle concentration of nitrogen adsorbed on pore surface, g.mole/(g. of adsorbent); q_o is the concentration on adsorbent in equilibrium with gas concentration C_o; q_∞ is the total adsorption capacity for monomolecular layer on adsorbent
q_1, q_2 = functions defined by Equations (33) and (34), cm.$^{-1}$ and sec.$^{-1}$, respectively
R = rate of adsorption at a point on the pore surface, g.mole/(sec.) (g. of adsorbent)
$\tilde{R}$ = overall rate of adsorption per unit volume of bed, g. mole/(sec.) (cc.)
r = radial distance from center of spherical particle, cm.
$\bar{r}$ = average pore radius, $2V/S$, cm.
S = pore surface area, sq. cm./(g. of adsorbent)
s = Laplace transform parameter for θ, sec.$^{-1}$
t = time, sec.; t_s is the time corresponding to an infinite rate of adsorption
V = void volume of Vycor particle, cc./(g. of adsorbent)
$W(s)$ = function of x defined by Equation (20)
x = distance coordinate defined by Equation (23), sec.$^{-1}$
$Y(s)$ = function of s defined by Equation (21), sec.$^{-1}$
z = axial distance in Vycor bed measured in direction of flow, cm.; z_o total length of packed bed
$\bar{z}$ = length of tubing measured from bed exit, cm.; z_o total length of tubing to detector

Greek Letters

α = defined by Equation (28), sec.$^{-1}$
γ = defined by Equation (29), sec.$^{-1}$
β = constant in Equation (31)
λ = integration parameter in Equation (25)
λ_e = adsorption constant, Kq_∞, cc./g.
ρ = density of gas mixture, g./(cc.); ρ_p = Vycor particle density, g./(cc.); ρ_B = density of packed bed of Vycor particles
ϵ_B = volume void fraction of bed (0.802); ϵ_p = void fraction of Vycor particles
μ = viscosity of gas mixture, g./(cm.) (sec.)
θ = time coordinate defined by Equation (24), sec.
ϕ = concentration as a function of time at the exit of the bed, g.moles/(cc.)

LITERATURE CITED

1. Anzelius, A. Z., *Angew. Math. und Mech.*, 6, 291-4 (1926).
2. Ballow, E. V., and O. K. Doolen, *Anal. Chem.*, **32**, 532 (1960).
3. Barrer, R. M., *J. Chem. Phys.*, **57**, 35 (1953).
4. ———, and J. A. Barrie, *Proc. Roy. Soc.*, **A213**, 250 (1952).
5. Bohart, G. S., and E. O. Adams, *J. Chem. Soc.*, **42**, 523 (1920).
6. Brunauer, S., "Physical Adsorption of Gases and Vapors," Vol. 1, Chapter 6, Oxford University Press, New York (1945).
7. Edeskuty, F. J., and N. R. Amundson, *J. Phys. Chem.*, **56**, 148 (1952).
8. Furnas, C. C., *Trans. Am. Inst. Chem. Engrs.*, **24**, 142 (1930).
9. Gamson, B. W., George Thodos, and O. A. Hougen, *ibid.*, **39**, 1-35 (1943).
10. Geser, J. J., and L. M. Canjar, *A.I.Ch.E. Journal*, **8**, 494 (1962).
11. Glueckauf, E., and J. I. Coates, *J. Chem. Soc.*, 1315 (1947).
12. Hiester, N. K., and Theodore Vermeulen, *Chem. Eng. Progr.*, **48**, 505 (1952).
13. Joyner, L. G., E. W. Weinberger, and C. W. Montgomery, *J. Am. Chem. Soc.*, **67**, 2182 (1945).
14. Marshall, W. R., Jr., and R. L. Pigford, "The Application of Differential Equations to Chemical Engineering Problems," Univ. of Delaware, Newark, Delaware (1947).
15. Rao, M. R., and J. M. Smith, *Ind. Eng. Chem.*, to be published.
16. Rosen, J. B., *J. Chem. Phys.*, **20**, 387 (1952).
17. Schumann, T. E. S., *J. Franklin Inst.*, **208**, 405 (1929).
18. Sillen, L. G., and E. Ekedahl, *Arkiv. Kemi. Mineral. Geol.*, **A22**, Nos. 15 and 16 (1946).
19. Thomas, H. C., *J. Am. Chem. Soc.*, **66**, 1664 (1944).
20. ———, *J. Chem. Phys.*, **19**, 1213 (1951).

Manuscript received March 6, 1963; revision received July 26, 1963; paper accepted July 30, 1963.